Metal-Driven Viscoelastic Wormlike Micelle in Anionic/Zwitterionic Surfactant Systems and Template-Directed Synthesis of Dendritic Silver Nanostructures

Yan Qiao,[†] Yiyang Lin,[†] Yijie Wang,[†] Zhibo Li,[‡] and Jianbin Huang*,[†]

[†]Beijing National Laboratory for Molecular Sciences (BNLMS), State Key Laboratory for Structural Chemistry of Unstable and Stable Species, College of Chemistry and Molecular Engineering, Peking University, Beijing 100871, China, and [‡]State Key Laboratory of Polymer Physics and Chemistry, Institute of Chemistry, Chinese Academy of Sciences, Beijing, 100190, PR China

In this work, metal ion-induced viscoelastic wormlike micelles in anionic/zwitterionic surfactant solutions (sodium dodecylsulfate/tetradecyldimethylammoniumpropanesulfonate, SDS/TPS) are reported. Steady and dynamic rheology and cryogenic transmission electron microscopy (cryo-TEM) are employed to characterize wormlike micelles in the SDS/TPS/Ca(NO$_3$)$_2$ system. Moreover, the surfactant mixing ratio and surfactant tail length are varied to reveal the factors that influence wormlike micelle growth and solution viscoelasticity. A series of metal ions such as Na$^+$, Mg^{2+}, Zn^{2+}, and Al^{3+} are proven to promote viscoelastic wormlike micelle formation in the SDS/TPS system. The metal-containing wormlike micelles are expected to be good candidates for directing the synthesis of inorganic nanomaterials. In this article, dendritic silver nanostructures have been prepared in the surfactant wormlike micelle by in situ UV irradiation for the first time.

Introduction

The molecular self-assembly of surfactants based on noncovalent interactions provides a powerful tool for the creation of well-defined structures in certain dimensions, such as vesicle, rod, fiber, disk, laminar structure, and 3D networks.[1] The 1D nanostructure has attracted extensive research interest over the past decade because of its significance in understanding biological self-assembly and appealing applications in nanoscience.[2] It is well known that surfactants can self-assemble into long, flexible, cylindrical chains with contour lengths of a few micrometers above a critical concentration. These 1D structures named "wormlike" or "threadlike" micelles are analogous to those observed in polymer solutions; therefore, they are also called equilibrium polymers or living polymers.[3] In some cases, an increase in end-cap energy combined with a decrease in the energy required to form a branch point would result in the formation of branched wormlike micelles.[4] These 1D structures typically become entangled into a transient network, thereby imparting viscoelastic properties to the solution. During the last few decades, viscoelastic wormlike micelles have drawn considerable interest from a theoretical viewpoint and for industrial and technological applications.[5] The fascinating structural characters and rheological properties render them useful in various applications such as viscosity enhancers, drag reduction agents, personal care products, and so on.

The most famous and studied wormlike micelle systems are cationic surfactants with long aliphatic chains, such as cetyltrimethylammonium bromide (CTAB) and cetylpyridinium bromide (CPBr), for which micellar growth takes place in the presence of an inorganic salt[6] or hydrotrope.[7] Mixtures of oppositely charged surfactants (referred to as catanionic systems) often exhibit a synergistic enhancement of rheological properties, for which micellar growth occurs by a decrease in the micellar surface potential via charge neutralization and an increase in ionic strength by the release of counterions.[8] Nonionic surfactant can

*Corresponding author. E-mail: jbhuang@pku.edu.cn. Fax: 86-10-62751708. Tel: 86-10-62753557.

(1) (a) Kaler, E. W.; Murthy, A. K.; Rodriguez, B.; Zasadzinski, J. A. N. *Science* **1989**, *245*, 1371. (b) Hao, J. C.; Hoffmann, H. *Curr. Opin. Colloid Interface Sci.* **2004**, *9*, 279. (c) Zemb, Th.; Dubios, M.; Demé, B.; Gulik-Krzywicki, Th. *Science* **1999**, *283*, 816. (d) Svenson, S. *Curr. Opin. Colloid Interface Sci.* **2004**, *9*, 201. (e) Fuhrhop, J.-H.; Helfrich, W. *Chem. Rev.* **1993**, *93*, 1565. (f) Qiao, Y.; Lin, Y. Y.; Yang, Z. Y.; Chen, H. F.; Zhang, S. F.; Yan, Y.; Huang, J. B. *J. Phys. Chem. B* **2010**, *114*, 11725.

(2) (a) Scheibel, T. *Curr. Opin. Biotechnol.* **2005**, *16*, 427. (b) Ross, C. A.; Poirier, M. A. *Nat. Med.* **2004**, S10. (c) Xia, Y. N.; Yang, P. D.; Sun, Y. G.; Wu, Y. Y.; Mayers, B.; Gates, B.; Yin, Y. D.; Kim, F.; Yan, Y. Q. *Adv. Mater.* **2003**, *15*, 353. (d) Lin, Y. Y.; Qiao, Y.; Gao, C.; Tang, P. F.; Liu, Y.; Li, Z. B.; Yan, Y.; Huang, J. B. *Chem. Mater.* **2010**, *22*, 6711.

(3) (a) Cates, M. E. *Macromolecules* **1987**, *20*, 2289. (b) Cates, M. E.; Candau, S. J. *J. Phys.: Condens. Matter* **1990**, *2*, 6869. (c) Rehage, H.; Hoffmann, H. *Mol. Phys.* **1991**, *74*, 933. (d) Acharya, D. P.; Kunieda, H. *Adv. Colloid Interface Sci.* **2006**, *123*, 401. (e) Gonzalez, Y. I.; Kaler, E. W. *Curr. Opin. Colloid Interface Sci.* **2005**, *10*, 256. (f) Walker, L. M. *Curr. Opin. Colloid Interface Sci.* **2001**, *6*, 451. (g) Magid, L. J. *J. Phys. Chem.* **1998**, *102*, 4064. (h) Trickett, K.; Eastoe, J. *Adv. Colloid Interface Sci.* **2008**, *144*, 66.

(4) (a) Danino, D.; Talmon, Y.; Lévy, H.; Beinert, G.; Zana, R. *Science* **1995**, *269*, 1420. (b) Bernheim-Groswasser, A.; Zana, R.; Talmon, Y. *J. Phys. Chem. B* **2000**, *104*, 4005. (c) Bernheim-Groswasser, A.; Wachtel, E.; Talmon, Y. *Langmuir* **2000**, *16*, 4131. (d) Zilman, A. G.; Safran, S. A. *Phys. Rev. E* **2002**, *66*, 051107.

(5) (a) Zakin, J. L.; Bewersdorff, H. W. *Rev. Chem. Eng.* **1998**, *14*, 2553. (b) Maitland, G. C. *Curr. Opin. Colloid Interface Sci.* **2000**, *5*, 301. (c) Abécassis, B.; Testard, F.; Zemb, Th. *Soft Matter* **2009**, *5*, 974.

(6) (a) Imae, T.; Abe, A.; Ikeda, S. *J. Phys. Chem.* **1988**, *92*, 1548. (b) Khatory, A.; Kern, F.; Lequeux, F.; Appell, J.; Porte, G.; Morie, N.; Ott, A.; Urbach, W. *Langmuir* **1993**, *9*, 933. (c) Candau, S. J.; Hirsch, E.; Zana, R.; Delsanti, M. *Langmuir* **1989**, *5*, 1225. (d) Khatory, A.; Lequeux, F.; Kern, F.; Candau, S. J. *Langmuir* **1993**, *9*, 1456. (e) Croce, V.; Cosgrove, T.; Maitland, G.; Hughes, T.; Karlsson, G. *Langmuir* **2003**, *9*, 8536. (f) Siriwatwechakul, W.; Lafleur, T.; Prud'homme, R. K.; Sullivan, P. *Langmuir* **2004**, *20*, 8970.

(7) (a) Shikata, T.; Hirata, H.; Kotaka, T. *Langmuir* **1987**, *3*, 1081. (b) Rehage, H.; Hoffmann, H. *J. Phys. Chem.* **1988**, *92*, 4712. (c) Clausen, T. M.; Vinson, P. K.; Minter, J. R.; Davis, H. T.; Talmon, Y.; Miller, W. G. *J. Phys. Chem.* **1992**, *96*, 474. (d) Carver, M.; Smith, T. L.; Gee, J. C.; Delichere, A.; Caponetti, E.; Magid, L. J. *Langmuir* **1996**, *12*, 691. (e) Soltero, J. F. A; Puig, J. E. *Langmuir* **1996**, *12*, 2654. (f) Hassan, P. A.; Valaulikar, B. S.; Manohar, C.; Kern, F.; Bourdieu, L.; Candau, S. J. *Langmuir* **1996**, *12*, 4350. (g) Cassidy, M. A.; Warr, G. G. *J. Phys. Chem.* **1996**, *100*, 3237. (h) Berret, J.-F. *Langmuir* **1997**, *13*, 2227. (i) Singh, M.; Ford, C.; Agarwal, V.; Fritz, G.; Bose, A.; John, V. T.; McPherson, G. L. *Langmuir* **2004**, *20*, 9931. (j) Lin, Y. Y.; Qiao, Y.; Yan, Y.; Huang, J. B. *Soft Matter* **2009**, *5*, 3047.

(8) (a) Koehler, R. D.; Raghavan, S. R.; Kaler, E. W. *J. Phys. Chem. B* **2000**, *104*, 11035. (b) Schubert, B. A.; Kaler, E. W.; Wagner, N. J. *Langmuir* **2003**, *19*, 4079. (c) Raghavan, S. R.; Fritz, G.; Kaler, E. W. *Langmuir* **2002**, *18*, 3797. (d) Hao, J.; Hoffmann, H.; Horbaschek, K. *Langmuir* **2001**, *17*, 4151.

also increase aqueous viscosity with the formation of elongated wormlike micelles.[9] Although micelle growth or the sphere-to-rod transition[10] has been extensively reported, wormlike micelles with markedly observable viscoelastic behavior in anionic[11] or zwitterionic[12] surfactant systems are found less frequently.

Herein, we report the formation of viscoelastic wormlike micelle solution in anionic/zwitterionic surfactant systems driven by a series of metal ions. The surfactants involved are anionic and zwitterionic, which are complementary to the majority of cationic wormlike micelle surfactants. Rheology and cryo-TEM analyses are performed to characterize surfactant wormlike micelles. The parameters that affect the solution rheological properties, such as the surfactant mixing ratio, surfactant tail length, and metal ion valence, are carefully discussed. It is worthwhile that the introduction of various metal ions, which are versatile in diverse subject areas, may endow the self-organized systems with versatile functionalities and novel properties. Particularly in the field of nanoscience, with a consideration of their structural similarity, wormlike micelles may be good candidates for directing 1D inorganic nanomaterials. The metal center can serve as both an inorganic precursor and a constituent of soft templates, which we described as a self-templating approach.[13] In our preliminary attempts, 1D silver dendrite nanostructures have been prepared by the direct reduction of silver ions by UV irradiation of the sodium dodecylsulfate/tetradecyldimethylammoniumpropane sulfonate/AgNO$_3$ (SDS/TPS/AgNO$_3$) wormlike micelle solution. As far as we known, dendritic silver nanostructures are synthesized for the first time in wormlike micelle systems. Dendritic silver nanostructures with 1D branches are anticipated to offer peculiar properties and further applications in the fields of catalysis, optics, surface-enhanced Raman scattering (SERS), and biosensors.[14]

Materials and Methods

Materials. Sodium dodecylsulfate (SDS, Acros, 99%), tetradecyldimethylammoniumpropane sulfonate (TPS, Fluka, ≥98%), dodecyldimethylammoniumpropane sulfonate (DPS, Fluka, ≥97%), nitrates, and other chemicals (Beijing Chemical Co., A.R. grade) were used as received.

Sample Preparation. Surfactant mixtures were prepared by mixing the individual surfactant solution directly in a test tube. Then the desired amount of a concentrated inorganic salt solution (0.5 or 1.0 M) was added to the tube with a microsyringe. After sealing, the sample was vortex mixed and equilibrated at high

temperature (~70 °C) for 1 h to ensure complete solubility and uniformity. The resulting mixture was maintained at 25.0 ± 0.5 °C in a thermostatted bath at least for 3 days before measurements.

Rheology Measurements. The rheological properties of the viscoelastic solution were measured at 25.00 ± 0.05 °C with a Thermo Haake RS300 rheometer (cone and plate geometry that is 35 mm in diameter with the cone gap equal to 0.105 mm). A solvent trap was used to avoid water evaporation. Frequency spectra were conducted in the linear viscoelastic regime of the samples determined from dynamic strain sweep measurements. For the sample with low viscosity, a double-gap cylindrical sensor system was used with an outside gap of 0.30 mm and an inside gap of 0.25 mm.

Cryo-TEM. Cryo-TEM samples were prepared in a controlled environment vitrification system (CEVS) at 25 °C. A small drop of sample was placed on a copper grid, and a thin film was produced by blotting off the redundant liquid with filter paper. This thin film was then quickly dipped into liquid ethane, which was cooled by liquid nitrogen. The vitrified samples were then stored in liquid nitrogen until they were transferred to a cryogenic sample holder (Gatan 626) and examined with JEM2200FS TEM (200 kV) at about −174 °C.

Preparation and Characterization of Dendritic Silver Nanostructures. In a typical synthesis, 5 mL of a silver-driven SDS/TPS wormlike micellar solution (C_T = 60 mM, X_{TPS} = 0.80, [AgNO$_3$] = 50 mM) is illuminated by ultraviolet light for 1 h. Then the transparent solution turns into yellow, and the viscoelastic fluid turned into a waterlike solution. The resulting solution was centrifugated to collect the precipitate at the bottom of the test tube. The black precipitate was washed with deionized water several times. The obtained precipitates were characterized by SEM (Hitachi S4800, 10 kV), TEM (JEOL JEM-200CX, 100 kV), HRTEM (FEI Tecnai F30, 300 kV), X-ray EDX (FEI Tecnai F30, 300 kV), and XRD (Rigaku Dmax-2000, Ni-filtered Cu Kα radiation). For the TEM and SEM measurements, the obtained products were dispersed in water and dropped onto a Formvar-covered copper grid and a silicon wafer, respectively, followed by drying naturally. For XRD measurements, several drops of the suspension were dropped onto a clean glass slide, followed by drying in air.

Results and Discussion

Ca^{2+}-Driven Viscoelastic Wormlike Micelle in the SDS/TPS System. The sodium dodecylsulfate/tetradecyldimethylammoniumpropane sulfonate (SDS/TPS, C_T = 60 mM) solution exhibits a low viscosity at all mixing ratios. However, with the addition of Ca(NO$_3$)$_2$, the waterlike solution turns into a viscoelastic fluid. As shown in Figure 1a, the SDS/TPS solutions (C_T = 60 mM, X_{TPS} = 0.50) exhibit a gradual viscosity enhancement with the increase in Ca(NO$_3$)$_2$ concentration. Herein, the TPS molar percentage, X_{TPS}, is defined as X_{TPS} = [TPS]/([SDS] + [TPS]). A viscosity increase can be also observed in the SDS/TPS mixture (X_{TPS} = 0.62) with the addition of Ca(NO$_3$)$_2$.

Steady and dynamic rheological measurements are performed to investigate the flow properties as the Ca(NO$_3$)$_2$ concentration increases at 25 °C. With increasing Ca(NO$_3$)$_2$ concentration, the surfactant system changes from a low-viscosity solution to a non-Newtonian fluid with high viscosity (Figure 1b). These samples exhibit a viscosity plateau at low shear rates and shear-shinning behavior at high shear rates. When the concentration of calcium ion reaches 10 mM, the low-shear viscosity of the surfactant solution can be as high as 4700 PaS, which is a nearly 6-fold enhancement. The dynamic rheological experiment indicates a viscoelastic response in the surfactant solution with the addition of Ca(NO$_3$)$_2$ (Figure 1c). When the calcium concentration is 6 mM, the sample shows liquidlike behavior ($G' < G''$) in the low-frequency region and solidlike behavior ($G' > G''$) in the

(9) (a) Jerke, G.; Pedersen, J. S.; Egelhaaf, S. U.; Schurtenberger, P. *Langmuir* **1998**, *14*, 6013. (b) Acharya, D. P.; Kunieda, H. *J. Phys. Chem. B* **2003**, *107*, 10168. (c) Sharma, S. C.; Acharya, D. P.; Aramaki, K. *Langmuir* **2007**, *23*, 5324.(d) Imanishi, K.; Einaga, Y. *J. Phys. Chem. B* **2007**, *111*, 62.

(10) (a) Missel, P. J.; Mazer, N. A.; Benedek, G. B.; Young, C. Y.; Carey, M. C. *J. Phys. Chem.* **1980**, *84*, 1044. (b) Alargova, R.; Petkov, J.; Petsev, D.; Ivanov, I. B.; Broze, G.; Mehreteab, A. *Langmuir* **1995**, *11*, 1530. (c) Alargova, R. G.; Danov, K. D.; Petkov, J. T.; Kralchevsky, P. A.; Broze, G.; Mehreteab, A. *Langmuir* **1997**, *13*, 5544. (d) Magid, L. J.; Li, Z.; Butler, P. D. *Langmuir* **2000**, *16*, 10028.

(11) (a) Hassan, P. A.; Raghavan, S. R.; Kaler, E. W. *Langmuir* **2002**, *18*, 2543. (b) Kalur, G. C.; Raghavan, S. R. *J. Phys. Chem. B* **2005**, *109*, 8599. (c) Kakamura, K.; Shikata, T. *Langmuir* **2006**, *22*, 9853. (d) Mu, J. H.; Li, G. Z.; Jia, X. L.; Wang, H. X.; Zhang, G. Y. *J. Phys. Chem. B* **2002**, *106*, 11685. (e) Angelescu, D.; Khan, A.; Caldararu, H. *Langmuir* **2003**, *19*, 9155. (f) Angelescu, D.; Caldararu, H.; Khan, A. *Colloids Surf., A* **2004**, *245*, 49. (g) Almgren, M.; Gimel, J. C.; Wang, K.; Karlsson, G.; Edwards, K.; Brown, W.; Mortensen, K. *J. Colloid Interface Sci.* **1998**, *202*, 222.

(12) (a) Hoffmann, H.; Rauschera, A.; Gradzielski, M.; Schulz, S. F. *Langmuir* **1992**, *8*, 2140. (b) Fischer, P.; Rehage, H.; Gruning, B. *J. Phys. Chem. B* **2002**, *106*, 1041. (c) Kumar, R.; Kalur, G. C.; Ziserman, L.; Danino, D.; Raghavan, S. R. *Langmuir* **2007**, *23*, 12849.

(13) Qiao, Y.; Lin, Y. Y.; Wang, Y. J.; Yang, Z. Y.; Liu, J.; Zhou, J.; Yan, Y.; Huang, J. B. *Nano Lett.* **2009**, *9*, 4500.

(14) (a) Rashid, M. H.; Mandal, T. K. *J. Phys. Chem. C* **2007**, *111*, 16750. (b) Wen, X.; Xie, Y.-T.; Mark, M. W. C.; Cheung, K. Y.; Li, X.-Y.; Renneberg, R.; Yang, S. *Langmuir* **2006**, *22*, 4836. (c) Lu, L.; Kobayashi, A.; Kikkawa, Y.; Tawa, K.; Ozaki, Y. *J. Phys. Chem. B* **2006**, *110*, 23234.
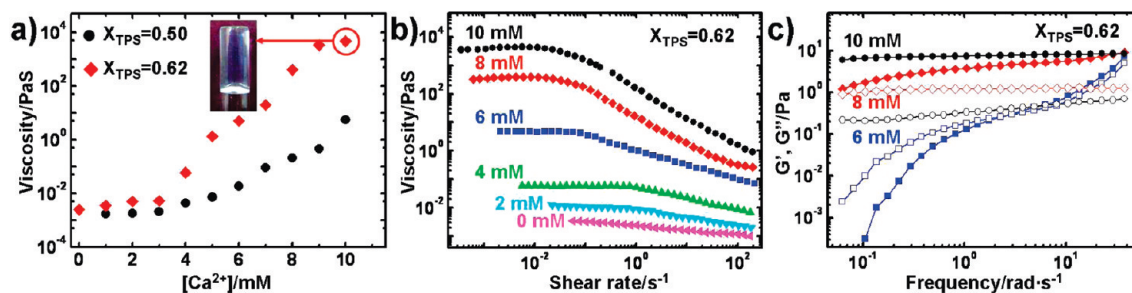
Figure 1. Influence of Ca(NO$_3$)$_2$ concentration on the rheological properties in SDS/TPS solution (C_T = 60 mM). (a) Zero-shear viscosity. (Inset) Gel-like fluid that satisfies the tube inversion test. The interior diameter of the tubes was 1.5 cm. (b) Steady shear viscosity. (c) Elastic modulus G' and viscous modulus G'' as functions of angular frequency ω.
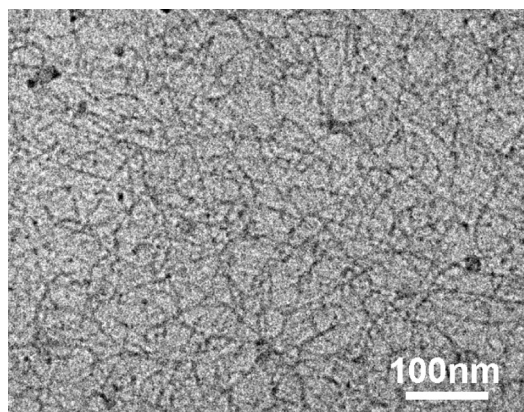
Figure 2. Cryo-TEM image of wormlike micelles in the SDS/TPS system (X_{TPS} = 0.62, C_T = 60 mM) in the presence of 6 mM Ca(NO$_3$)$_2$.

Scheme 1. Schematic Mechanism of Wormlike Micelle Formation in the SDS/TPS/Ca(NO$_3$)$_2$ System

high-frequency region. The viscoelastic response may be caused by the formation of wormlike micelles. The elastic modulus $G'(\omega)$ and the viscous modulus $G''(\omega)$ exhibit a crossover at an angular frequency of ω = 20 rad/s, of which the inverse is often used to determine the relaxation time. Further increases in calcium ion concentration to 8 mM lead to a more remarkably viscoelastic fluid with a lower crossover frequency (ω = 0.06 rad/s). More interestingly, when the calcium concentration reaches 10 mM, the dynamic oscillation curve shows no crossover frequency, which indicates an infinite relaxation time. From a rheological stand-point, wormlike micelles typically exhibit a viscoelastic response with a finite relaxation time. In this regard, the rheology of this system is qualitatively different from that of wormlike micelles but is true for "permanent" gels in which the dynamic moduli remain nonzero at low frequencies and the elastic modulus $G'(\omega)$ exceeds the viscous modulus $G''(\omega)$ over the entire range of frequencies. This rheology is reminiscent of a cross-linked gel rather than an entangled network of wormlike chains. Similar results have been reported by Raghavan in EHAC/NaSal and zwitterionic EDAB systems in which the surfactant possesses a C$_{22}$ hydrocarbon chain. Actually, the gel-like viscoelastic fluid even satisfies the tube inversion test (inset of Figure 1a).[15,12c]

Cryogenic transmission electron microscopy (cryo-TEM) is employed for the direct visualization of micelle morphology, which can help correlate microstructure to macroscopic rheological behavior in a surfactant solution. As indicated in Figure 2, a large number of elongated flexible wormlike micelles are evidenced in SDS/TPS solution in the presence of 6 mM Ca(NO$_3$)$_2$. The micelle diameter is about 5 nm, which is comparable to double the extended length of the surfactant molecule (about 25 Å). These micelles can reach to hundreds of nanometers or even several micrometers in length and are found to overlap with each other and entangle into 3D network structures. This is the reason for the observable viscoelasticity in SDS/TPS/Ca(NO$_3$)$_2$ solution as discussed above.
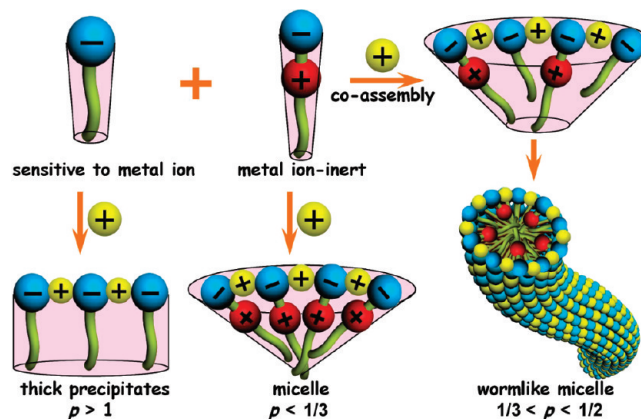
Explanation of Wormlike Micelle Formation in the SDS/TPS/Ca(NO$_3$)$_2$ System. It is well known that multivalent metal ions interact intensely with SDS or even result in thick precipitates because of the strong electrostatic attraction between metal ions and anionic headgroups. For example, precipitates are obtained in 60 mM SDS solution with the addition of a subtle amount of Ca(NO$_3$)$_2$ (>6 mM). Oppositely, zwitterionic surfactants are known to be salt-inert owing to the lack of negative net charge on the surfactant headgroup.[16] However, the situation is very interesting in the anionic/zwitterionic surfactant solution (SDS/TPS) in the presence of Ca(NO$_3$)$_2$ in which viscoelastic wormlike micelles are formed. A schematic mechanism is presented in Scheme 1. It is proposed that the electrostatic repulsive force between charged surfactant groups in SDS/TPS micelles will result in loose surfactant packing and prevent the formation of viscoelastic wormlike micelles although a synergic interaction may exist between anionic and zwintterionic surfactants. The association of Ca^{2+} with the anionic headgroup can reduce the repulsive force between surfactant headgroups. Meanwhile, divalent metal ions are expected to bridge the adjunction anionic surfactant through electrostatic attraction. Both of these factors can bring about the close packing of the SDS/TPS/Ca^{2+} complex in aggregates and increase the critical packing parameter (p) of the

(15) Raghavan, R. S.; Kaler, E. W. *Langmuir* **2001**, *17*, 300.

(16) (a) Chorro, M.; Kamenka, N.; Faucompre, B.; Partyka, S.; Lindheimer, M.; Zana, R. *Colloids Surf., A* **1996**, *110*, 249. (b) Kamenka, N.; Haouche, G.; Brun, B.; Lindman, B. *Colloids Surf.* **1987**, *25*, 287.
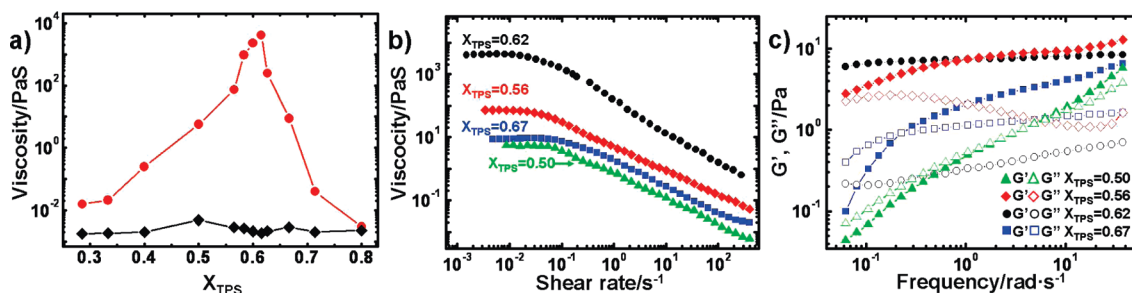
Figure 3. Effect of TPS molar percentage on the rheological properties of the SDS/TPS system (C_T = 60 mM, [Ca(NO$_3$)$_2$] = 10 mM). (a) Zero-shear viscosity profile, with (red circle) and without (black diamond) Ca(NO$_3$)$_2$. (b) Steady shear viscosity curve. (c) Elastic modulus G' and viscous modulus G'' as functions of the angular frequency.
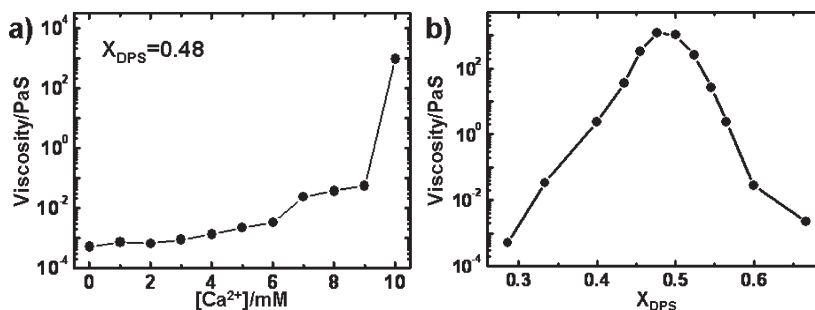
Figure 4. (a) Zero-shear viscosity of the SDS/DPS/Ca^{2+} system as a function of Ca(NO$_3$)$_2$ concentration (C_T = 60 mM, X_{DPS} = 0.48). (b) Zero-shear viscosity of SDS/DPS/Ca^{2+} as a function of the DPS molar percentage (C_T = 60 mM, [Ca(NO$_3$)$_2$] = 10 mM).

SDS/TPS system, as a result of which elongated wormlike micelles are formed ($^1/_3$ < *p* < $^1/_2$).[17]

Parameters Influencing the Rheological Properties of the SDS/TPS/Ca(NO$_3$)$_2$ Mixture. *Surfactant Molar Percentage.* The effect of TPS molar percentage X_{TPS} on the rheological properties of the SDS/TPS/Ca(NO$_3$)$_2$ solution is studied. The total surfactant concentration is fixed at C_T = 60 mM. In the absence of Ca(NO$_3$)$_2$, SDS/TPS mixtures exhibit low viscosity at all mixing ratios (Figure 3a). With the addition of 10 mM Ca(NO$_3$)$_2$, the solution viscosity is greatly enhanced. As Figure 3a shows, the viscosity profile ascends initially as X_{TPS} increases, followed by a sharp decrease. There exists an optimal surfactant composition of X_{TPS} = 0.62 at which the solution viscosity reaches its maximum (i.e., the micelles reach their maximum growth). The steady shear plot is presented in Figure 3b, which demonstrates the shear-thinning behavior with the highest viscosity at X_{TPS} = 0.62. The dynamic oscillation curve in Figure 3c shows that the elastic modulus G' and viscous modulus G'' can be detected in SDS/TPS/Ca(NO$_3$)$_2$ solution at different TPS percentages (X_{TPS} = 0.50−0.67). The highest elastic modulus and viscous modulus are observed at X_{TPS} = 0.62, which is in agreement with the steady rheological result. We have proposed that the binding of calcium ions to anionic surfactant headgroups can effectively suppress the electrostatic repulsive interactions and lead to micelle growth. When X_{TPS} is lower than 0.62, SDS is present in excess and the electrostatic repulsive force is not completely screened by 10 mM Ca(NO$_3$)$_2$. As a result, the solution viscosity rises with the increase in TPS percentage or the decrease in SDS percentage. When X_{TPS} is higher than 0.62, zwitterionic surfactant TPS is dominant, which may restrict the close packing of surfactants and lowers the value of the critical packing parameter.[16] As a result, wormlike micelles are shortened and the solution viscoelasticity is weakened.

(17) (a) Nagarajan, R. *Langmuir* **2002**, *18*, 31.(b) Israelachvili, J. N. *Intermolecular and Surface Forces*; Academic Press: New York, 1992. (c) Wabel, C. Ph.D. Dissertation, University of Erlangen, 1998.

Surfactant Structure. To investigate the effect of surfactant structure on rheology and micelle growth, the sodium dodecyl-sulfate/dodecyldimethylammoniumpropane sulfonate (SDS/DPS) system is studied. Compared with TPS, zwitterionic surfactant DPS has the same headgroup but a shorter C12 hydrocarbon chain. As shown in Figure 4a, Ca(NO$_3$)$_2$ can also induce viscosity enhancement in the SDS/DPS solution (C_T = 60 mM, X_{DPS} = 0.48). When the concentration of Ca(NO$_3$)$_2$ reaches 10 mM, the low shear viscosity of the surfactant solution can be as high as 1200 PaS, which is 6 orders of magnitude greater than for the SDS/DPS solution without calcium ions. Figure 4b shows the zero-shear viscosity of SDS/DPS/Ca^{2+} as a function of the DPS molar percentage (C_T = 60 mM, [Ca(NO$_3$)$_2$] = 10 mM). The following can be noticed from Figure 4b: (1) The system also exhibits a viscosity maximum in the profile in which the viscosity peak of the SDS/DPS system occurs at X_{DPS} = 0.48. (2) The maximum solution viscosity of the SDS/DPS/Ca^{2+} solution is relatively lower than that of the SDS/TPS/Ca^{2+} solution. This is because DPS has a shorter hydrocarbon tail than TPS and consequently the aggregating capability of DPS is weaker.

Viscoelastic Wormlike Micelles in SDS/TPS Solution Caused by Different Metal Ions. It is worthwhile that viscoelastic wormlike micelle can be designed in the SDS/TPS system with the addition of various metal ions (Figure 5). For example, a series of bivalent cations including Mg^{2+}, Sr^{2+}, Ba^{2+}, Pb^{2+}, Cu^{2+}, Zn^{2+}, and Cd^{2+} can induce wormlike micelle in the SDS/TPS solution. Also, a number of monovalent ions such as Na$^+$, K$^+$, and Ag$^+$ and trivalent inorganic ions such as Al^{3+} and La^{3+} have also been found to enhance the solution viscosity.

From the results of Figures 5 and 6, the efficiency of viscosity enhancement by different metal ions is compared. It is noted that monovalent metal ions such as Na$^+$ are not efficient enough to enhance the solution viscosity. In the SDS/TPS/NaNO$_3$ system (C_T = 60 mM, X_{TPS} = 0.50), only when the sodium ion concentration reaches 150 mM can the solution viscosity rise to 1000 PaS

 1721
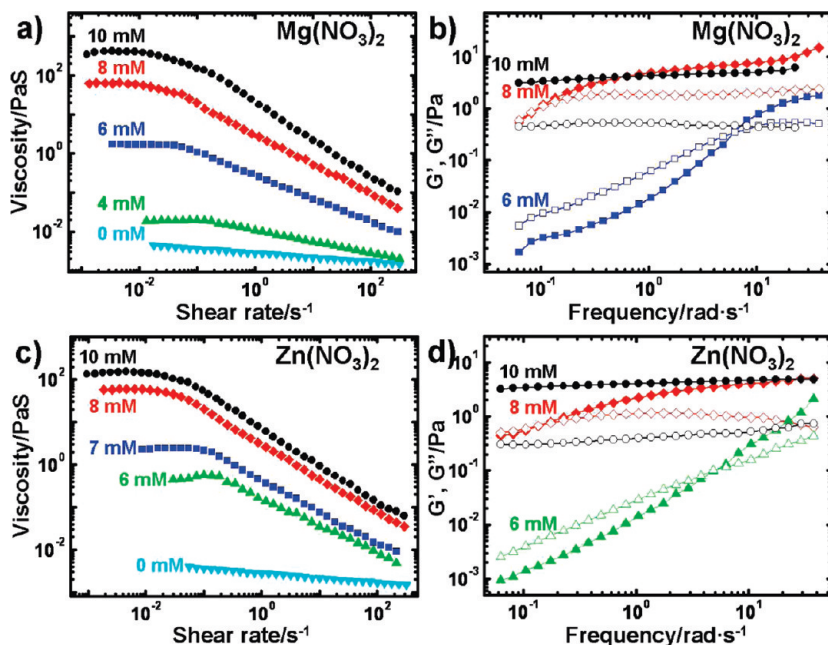
Figure 5. Solution viscosity of SDS/TPS systems in the presence of different bivalent metal ions: (a, b) Mg^{2+}(c, d) and Zn^{2+}. (a, c) Steady shear viscosity plot. (b, d) Dynamic oscillation curve.

Figure 6. Rheological curve of SDS/TPS systems in the presence of (a, b) $NaNO_3$ and (c, d) $Al(NO_3)_2$. (a, c) Steady shear viscosity plot. (b, d) Dynamic oscillation curve.

(Figure 6a). On the contrary, fewer divalent metal ions are needed to give viscoelastic wormlike micelles in the SDS/TPS solution. For example, the solution viscosity can rise to 1000 PaS with the addition of only 10 mM Mg^{2+} and Zn^{2+} (Figure 5a,c). Trivalent metal ion Al^{3+} is shown to be the most efficient in enhancing solution viscoelasticity (Figure 6c). This is because multivalent metal ions interact strongly with anionic species through Coulomb interactions and bridging effects In contrast, monovalent metal ions such as Na^+ and K^+ are not very efficient at inducing wormlike micelle formation.

Template-Directed Synthesis of Silver Dendrites. As mentioned above, wormlike micelles can be formed in anionic/zwitterionic surfactant systems with the addition of different metal ions. It is envisioned that the metal-containing wormlike micelles can be transformed into inorganic nanomaterials by a self-templating approach that we referred to previously.[13] The metal ions in this system can serve as both inorganic precursors and constituents of the template. As a preliminary attempt, the silver-driven wormlike micellar solution in the SDS/TPS system (C_T = 60 mM, X_{TPS} = 0.80, $[AgNO_3]$ = 50 mM) is used to synthesize the silver nanomaterial. Steady and dynamic rheology (Figure 7a) confirms the formation of wormlike micelles in the SDS/TPS/$AgNO_3$ system with a zero-shear viscosity of 0.02 PaS and a viscoelastic response. The direct visualization of wormlike micelles is obtained by cryo-TEM. Figure 7b represents a typical network of wormlike micelles in which these aggregates overlap
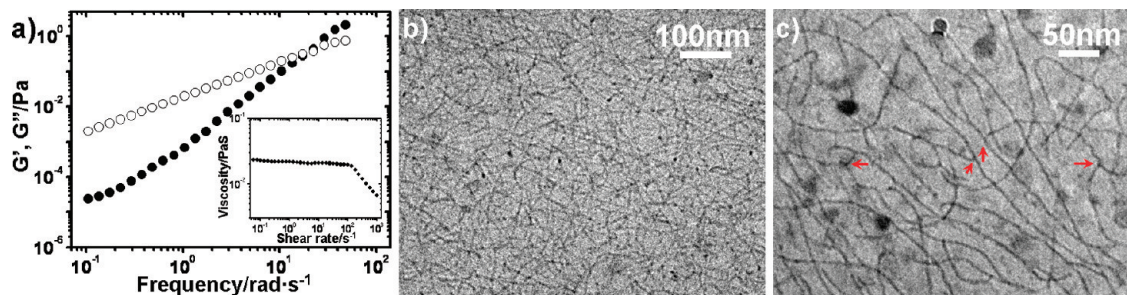
Figure 7. (a) Dynamic rheology curve of the SDS/TPS/AgNO$_3$ system (C_T = 60 mM, X_{TPS} = 0.80, [AgNO$_3$] = 50 mM). A steady shear viscosity plot is shown in the inset. (b) Cryo-TEM image and (c) high-magnification cryo-TEM image.
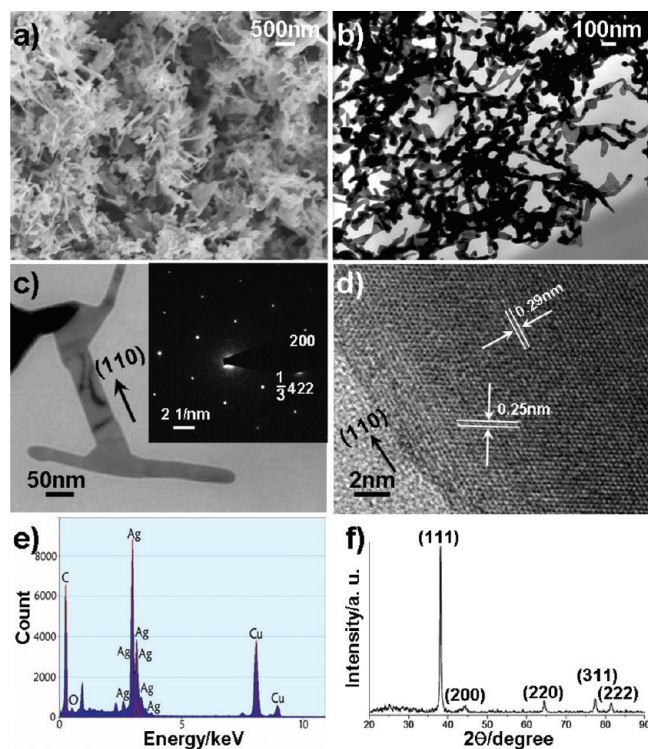
Figure 8. Dendritic Ag nanostructures as prepared: (a) SEM image, (b) TEM image, (c) TEM image of an individual silver branch and an ED pattern (inset), (d) typical HRTEM image, (e) EDS data, and (f) XRD spectrum.

and become entangled. In a magnified image, a number of Y junctions are observed (Figure 7c, indicated by red arrows), which means that some of the wormlike micelles are branched. After being illuminated with ultraviolet light for 1 h, the transparent solution turns yellow. The color change indicates the generation of nanosized inorganic silver materials. Figure 8a shows a representative low-magnification SEM image of the silver product, which consists of dendrite structure with a 1D branch. The EDS (Figure 8e) and XRD patterns (Figure 8f) of the silver dendrite exhibit pure, well-crystallized cubic Ag (JCPDS 04-0783). A TEM image shown in Figure 8b clearly shows that the dendrite nanostructures typically range from 20 to 100 nm in width. The

morphology of silver dendrite is in good agreement with the organic template, which is a network of branched 1D structures (Figure 8c). The selected-area electron diffraction (SAED) pattern (Figure 8c, inset) of an individual branch can be indexed to the [$\bar{1}$11] zone axis of cubic silver, indicating that the branch is a single crystal grown along the [110] direction and enclosed by the {211} and {111} planes as the side and top surfaces, respectively. The appearance of weak spots corresponds to the forbidden ($^1/_3$){422} reflection. A typical HR-TEM image is shown in Figure 8d, which exhibits clear fringes with a spacing of 0.29 nm due to the (110) reflection and a spacing of 0.25 nm that is responsible for the ($^1/_3$){422} reflection, confirming that each Ag branch is a [110]-oriented single crystal. To the best of our knowledge, this is the first report of a silver dendrite synthesized in a surfactant wormlike micelle system. It is hoped that a series of inorganic nanomaterials can be designed on the basis of this system.

Conclusions

Metal-induced viscoelastic wormlike micelles in anionic/zwitterionic surfactant systems are reported. In a typical case, Ca(NO$_3$)$_2$ is found to drive the formation of elongated wormlike micelles in the SDS/TPS system and the parameters affecting the rheological properties are systematically investigated. It is found that there exists a maximum solution viscosity by varying the surfactant composition (X_{TPS}) at a certain surfactant concentration, and elongating the surfactant hydrophobic tail can promote wormlike micelle growth. It is worthwhile that a series of metal ions are proven to drive wormlike micelle formation, and the efficiency sequence is Al^{3+} > Ca^{2+}, Mg^{2+}, Zn^{2+} > Na$^+$. Finally, the wormlike micelles in SDS/TPS/AgNO$_3$ are exploited to synthesize the silver dendrite nanomaterial in which metal ions serve as both inorganic precursors and constituents of the template. It is anticipated that metal-driven viscoelastic wormlike micelle systems are appealing soft templates for the preparation of various inorganic nanomaterials. We also hope that this study may shed a light on the fabrication of metal−organic hybrid materials and the versatile application of wormlike micelles.